

INSTRUMENTED FIELD DATA-BASED ASSESSMENT ON LOAD TRANSFER BEHAVIOR IN RAMMED AGGREGATE PIER® (RAP) ELEMENTS

Ece KURT BAL^{1*}, Mustafa Kubilay KELEŞOĞLU², Kemal Önder ÇETİN³

¹ Istanbul University-Cerrahpasa, Faculty of Engineering, Department of Civil Engineering, Istanbul, Türkiye

ORCID No: <https://orcid.org/0000-0003-2889-5881>

² Istanbul University-Cerrahpasa, Faculty of Engineering, Department of Civil Engineering, Istanbul, Türkiye

ORCID No: <https://orcid.org/0000-0003-1721-7946>

³ Middle East Technical University, Faculty of Engineering, Department of Civil Engineering, Ankara, Türkiye

ORCID No: <https://orcid.org/0000-0003-0540-2247>

Keywords

Rammed Aggregate Pier®,
Loading Test,
Instrumentation,
Load Transfer

Abstract

Among the methods of stone column installation, the use of Rammed Aggregate Pier® (RAP) elements offers an alternative to traditional methods like deep foundations or excavation/backfill for sites with challenging soil conditions that cannot meet the performance criteria of superstructures. The goal of using RAP elements is to reduce settlements to acceptable levels, increase load-bearing capacity, and minimize liquefaction potential. In this study, full-scale field load test was performed to identify the variation of shear resistance along RAP element installed by the Impact® System (displacement), making this research the first and only study conducted on RAP elements produced using the displacement system. More specifically, load cells were used to assess the mobilization of vertical load distribution along the column. By utilizing these load cells positioned at various levels along the column, the axial load distribution was monitored concurrently during the loading test. Full-scale load test results demonstrated that, under a 57.5 ton load, the displacement measured at the tell-tale element (reading bars mounted on load cells) varied relative to the displacement measured at the top level of the column, by approximately 15% at the 1 m level, and in the other levels (2 m, 4 m, and 6 m) by about 2-5%. When these results were evaluated in terms of the literature-defined settlement ratio ($R_b \gg 1$), the measured displacements indicated that the response was governed by lateral expansion of the column. Furthermore, the load cells indicated that the applied load mobilized rapidly up to the 1 m level ($\sim 2D$; D : pier diameter), with only about 10% of the load being transmitted; in other words, the load was accommodated predominantly by circumferential friction rather than transmission to the column tip. These findings support a deformation mechanism for RAP elements with $L/D \gg 3.5$ (L : pier length) that is driven by circumferential friction rather than tip capacity.

DARBELİ KIRMATAŞ KOLON® (DKK) ELEMANLARINDA YÜK TRANSFER DAVRANIŞININ ENSTRÜMANTASYONLU SAHA VERİ TABANLI DEĞERLENDİRİLMESİ

Anahtar Kelimeler

Darbeli Kırmataş Kolon®,
Yükleme Testi,
Enstrümantasyon,
Yük Transferi

Öz

Taş Kolon imalat yöntemleri arasında yer alan ve üst yapı performans kriterlerini karşılayamayacak özelliklere sahip olan zeminlerde derin temel ya da kazı/dolgu gibi mevcut yöntemlere alternatif olan Darbeli Kırmataş Kolon® (DKK) elemanları ile oturumaların uygun seviyelere indirilmesi, taşıma kapasitesinin artırılması ve sivilleşme potansiyelinin azaltılması hedeflenmektedir. Bu çalışmada, enstrümantasyonlu DKK elemanı üzerinde gerçekleştirilen tam ölçekli yüklem testi sonuçları değerlendirmeye alınmış olup, bu araştırma Impact® Sistemi (displacement) ile imal edilen Darbeli Kırmataş Kolon® elemanlarındaki yük mobilizasyonunun anlaşılmasına yönelik yürütülen ilk ve tek çalışma niteliğindedir. Bu kapsamda özel olarak tasarlanan ve kolonun farklı kademelerine yerleştirilen yük hücreleri ile yüklem testi sırasında ölçümler yapılarak kolon boyunca mobilize olan eksenel yük dağılımı eşzamanlı olarak ölçülmüştür. Tam ölçekli yüklem testi sonuçları, 57.5 ton yüklem altında tell-tale (yük hücrelerine monte edilmiş okuma çubukları) elemanlarında ölçülen deplasmanın, kolon üst kotunda ölçülen deplasmana göre 1 m seviyesinde yaklaşık %15'i, diğer seviyelerde



Bu eser, Creative Commons Attribution License (<http://creativecommons.org/licenses/by/4.0/>) hükümlerine göre açık erişimli bir makaledir.

This is an open access article under the terms of the Creative Commons Attribution License (<http://creativecommons.org/licenses/by/4.0/>).

(2 m, 4 m ve 6 m) ise %2-5'i aralığında değiştiğini göstermiştir. Elde edilen bu sonuçlar literatürde tariflenen oturma oranı ($R_b \gg 1$) cinsinden de değerlendirildiğinde ölçülen deplasmanların kolonun yanal genişlemesinden kaynaklı olduğunu göstermiştir. Ayrıca yük hücreleri, uygulanan yükün 1 m seviyelerinde ($\sim 2D$; D: kolon çapı) hızla mobilize olduğunu ve bu seviyelere yükün ancak %10'unun iletildiğini; başka bir ifade ile yükün kolon ucuna aktarılmadan çevre sürtünmesi ile karşılandığını göstermiştir. Bu sonuçlar, $L/D \gg 3.5$ (L: kolon boyu) olan DKK elemanlarının, uç kapasitesinden ziyade çevre sürtünmesine dayalı olan çalışma prensibini de destekler mahiyette bulunmuştur.

Araştırma Makalesi		Research Article	
Başvuru Tarihi	: 16.06.2025	Submission Date	: 16.06.2025
Kabul Tarihi	: 11.12.2025	Accepted Date	: 11.12.2025

* Sorumlu yazar: ekurt@sentezinsaat.com.tr
<https://doi.org/10.31796/ogummf.1719084>

1. Introduction

Ground improvement techniques have become essential in modern geotechnical engineering to enhance the bearing capacity, settlement and stability of soft or problematic soil profiles, ensuring the safe support of overlying structures. Among these techniques, Rammed Aggregate Pier® (RAP) elements have gained significant attention due to their efficiency, versatility, and high performance in various soil conditions. RAP elements, as documented in the literature (e.g., Lawton and Fox, 1994; Wissmann and Fox, 2000), are highly effective in improving soft soil profiles to support structures by increasing bearing capacity and reducing soil deformations under monotonic or cyclic loading (e.g., Lawton, Fox, and Handy, 1994; Wissmann, Moser, and Pando, 2001).

Additionally, they play a critical role in mitigating liquefaction risks in sandy and silty soils (e.g., Wissmann, Ballegooy, Metcalfe, Dismuke and Anderson, 2015). Similarly, RAP technology, rooted in traditional stone column design principles, has emerged as a preferred method in recent years due to its superior installation performance and speed. The distinguishing feature of RAP lies in its installation technology, which provides 2-9 times greater stiffness compared to other stone column methods (White, Wissmann, Barnes, and Gaul, 2002), making it a robust solution for ground improvement. The design and performance of both rammed aggregate piers and stone columns are influenced by several critical factors. The design of aggregate piers hinges on their capacity to endure applied loads and stresses while minimizing deformations in the forms of bulging and settlements. These elements also ensure the integrity of the composite soil-aggregate pier system by keeping overall settlements within permissible limits. The stress transfer mechanism between the piers and the surrounding soil is a fundamental aspect that influences their performance, requiring detailed investigation to optimize design approaches. For stone columns, the capacity and deformation behavior are

significantly influenced by the installation method, more specifically, the type of compaction process employed -whether vertical or horizontal vibration. Traditional methods, such as vibro-compaction and vibro-displacement systems (wet/dry, top/bottom feed), rely on horizontal vibration for compaction (John, Tim, Hilary, and Michael, 2012). In contrast, RAP systems, utilize vertical vibration, where an impact hammer compacts the aggregate vertically while also densifying the surrounding soil laterally. Vertical vibration techniques have been proposed to modify the passive earth pressure coefficient, with findings indicating that initial earth pressure coefficient (K_0) tends to approach the Rankine passive earth pressure coefficient (K_p) as a result of installation effects (Handy and White, 2006). RAP elements are constructed employing high-frequency impacts instead of horizontal vibrations. This method involves densifying the soil in thin layers, applying pre-strain and pre-stress, which results in highly dense and stiff foundation elements due to increased confining stresses that significantly minimize vertical displacements under foundation loads.

The design procedures for stone columns have advanced significantly since the 1960s, with early approaches focusing on bearing capacity and settlement-based methodologies. Over the past decade, the integration of field data and theoretical models with numerical methods has further refined these design practices, enhancing their reliability and applicability. Given the growing popularity of RAP elements as soil improvement solutions, understanding their design principles, stress transfer mechanisms, and performance under various loading conditions has become more critical than ever.

This research aims to explore the mechanisms of stress distribution in Rammed Aggregate Pier® elements constructed by the Impact® System (displacement) which utilizes 3-up-2-down compaction procedure. It also compares these experimental results with existing literature to provide comprehensive insights into their

performance when subjected to vertical loads, which in turn is hoped to contribute to the optimization of their design and application in geotechnical engineering.

As part of this framework, a specialized load cell has been designed to enable the placement of the RAP element at different levels of the pier. This design aims to elucidate whether the applied load is transmitted along the column primarily through circumferential friction along its length or whether it is transmitted to the column tip, thereby revealing the column behavior.

Although the literature includes studies aimed at understanding load mobilization for RAP elements installed with the replacement system, this study represents the first and pioneering investigation developed to elucidate the load transfer mechanism of RAP elements produced using the displacement system.

2. Literature Review

Rammed Aggregate Pier® elements are extensively utilized in geotechnical practice, serving as a key method for enhancing the bearing capacity of weak soil conditions. The integrated system comprising the pier and surrounding soil by this process reduces the compressibility of the soil and mitigate the excessive settlement under applied loads. Additionally, the piers promote radial drainage, accelerating the consolidation process in cohesive soils and further contributing to improved shear strength, stability and liquefaction potential. Furthermore, the vibration and volumetric densification during RAP installation are anticipated to enhance the strength and rigidity of non-cohesive soils, such as sandy, gravelly, or low-plasticity silty materials. By installing compacted layers through vertical ramming action into the soft/loose soil matrix, the upper structure loads are effectively distributed within the treated zone. The effectiveness of load transfer into the improved zone primarily relies on the lateral support stress exerted by the adjacent soil.

Extensive research has been performed on the failure mechanisms of stone columns, primarily employing limit equilibrium approaches to assess bearing capacity under specific failure modes (Greenwood, 1970; Vesic, 1972; Hughes and Withers, 1974; Wong, 1975; Madhav and Vitkar, 1978; Barksdale and Bachus, 1983).

The bearing capacity of RAP supported footings is typically limited by settlement, but excessive pressure can trigger yield in the improved soil, reaching its limit equilibrium capacity. In unimproved soils, shear failure surfaces are generally presumed to develop along circular paths or logarithmic spiral paths beneath the foundation. RAP-improved soil exhibits complex failure due to interactions between rigid piers and weaker surrounding soil. Possible failure modes illustrated in Figure 1 are categorized into four distinct types: a)

Bulging of individual piers; b) Shear failure under pier tips; c) Shearing within the pier-soil interface; d) Shearing below the improved soil zone (Wissmann, 1999).

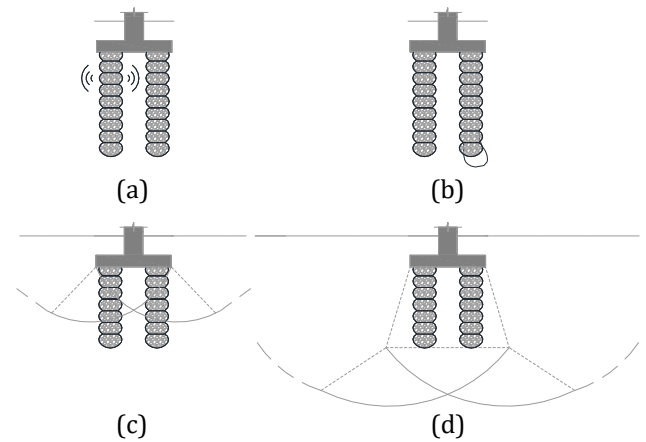


Figure 1. Potential Failure Modes for Rammed Aggregate Pier® (RAP) Elements (Wissmann, 1999).

Mitchell (1981) describes bulging failure in stone columns within saturated clays (Figure 1a), where applied pressure mobilizes shear strength, causing outward bulging, primarily in the upper portions due to lower lateral earth pressure near the surface. Evaluative techniques for single columns in soft cohesive soils assume a three-dimensional stress state, with lateral confining stress considered the ultimate passive resistance provided by the adjacent soil playing a critical role in supporting the column. Bulging failure, where the column deforms laterally under vertical load, is common for long columns bearing on a stiff stratum. The potential for shear failure beneath the base of individual RAP elements, as shown in Figure 1b, occurs when the total load transfers to the tip of insufficiently long columns (Barksdale and Bachus, 1983; McKelvey, Sivakumar, Bell and Graham, 2004; Suleiman and White, 2006).

The potential of shearing within the RAP-improved soil, as shown in Figure 1c, involves shear planes passing through the piers and surrounding soil, with the shear strength determined by the frictional resistance of the matrix soil and RAP elements.

Shearing below the RAP-improved soil matrix (Figure 1d) is evaluated by analyzing stresses at the foundation of the improved layer estimated using a 2:1 load spread, with the allowable bearing pressure (NAVFAC, 1983), with results for typical parameters provided.

Ultimately, the bearing capacity depends on column diameter, and the rigidity and strength of both the pier and surrounding soil, influenced by pier length having a negligible effect on long columns. This is supported by model tests indicating most of the applied load is primarily transmitted to the surrounding soil instead of

the pier base (Hughes and Withers, 1974). This load transfer mechanism has been validated through field and laboratory tests, emphasizing the importance of soil column interaction.

Hughes and Withers (1974) investigated the decaying stress responses with depth in stone column elements through a model test. Figure 2 shows the variation of vertical stresses with depth, where the stress decreases from a maximum ultimate value at the top during bulging failure to zero at 6 m depth. This study shows that increasing the column length beyond a certain value (6 meters for their particular setup) does not enhance the column's strength. When the column length is reduced, part of the applied vertical stress is transmitted to the soil at the tip, causing the columns to behave partially like end-bearing piles. If the columns are shortened sufficiently so that the base stress exceeds the soil's bearing capacity, end-bearing failure occurs before bulging of columns start.

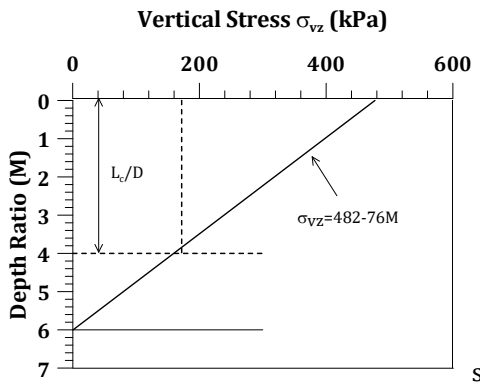


Figure 2. Vertical Stress Distribution in the Model Stone Column (Hughes and Withers, 1974).

The vertical stress distributions at different load increments, measured from total-stress cells embedded in the shafts of the replacement piers, are presented in Figure 3 and Figure 4. In White et al. (2007), the RAP length was chosen as 2.97 m, while in Gamboa (2022) it is tested as 4.2 m.

For a 2.97 m long RAP, White et al. (2007) indicated that under 240 kN vertical load, the vertical stress is reduced to 18% of its value at the top of the elements at a depth of 2.3 meters, while Gamboa (2022) reported that under 255 kN the same depth experiences roughly a 15% of the stresses applied at the top.

The vertical-stress variations are nonlinear and they decay rapidly with depth within couple of diameters of the element, indicating that a significant portion of pier cap loads are transmitted to host soils via shaft shear below the pier cap depth.

Overall, the load transfer mechanism of stone columns, which depends on their stiffness, lateral soil

confinement, and radial load spreading, provides an efficient solution for strengthening soft soil foundations.

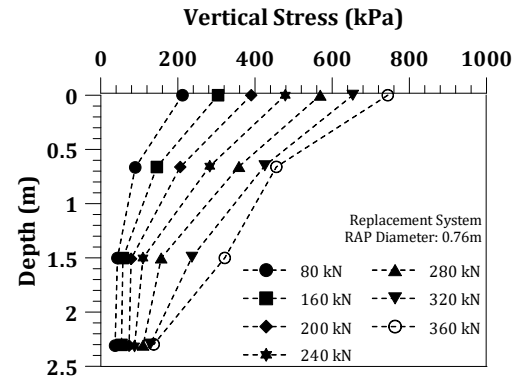


Figure 3. Measurements of Vertical Stress Increase Along Pier Shaft (White et al., 2007).

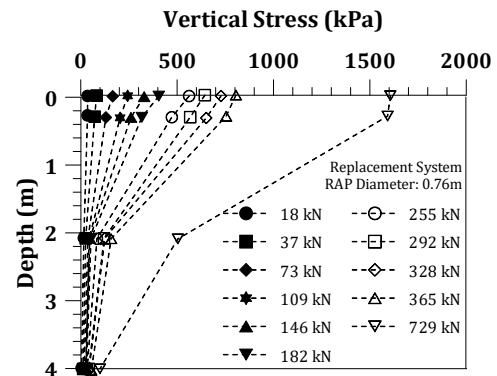


Figure 4. Measurements of Vertical Stress Increase Along Pier Shaft (Gamboa, 2022).

3. Methodology

To further investigate this load transfer mechanism, a well-instrumented Impact® Rammed Aggregate Pier® (RAP) was designed to assess the load distribution along the pier. A specialized load cell, engineered to withstand compacted aggregate conditions and capable of simultaneous data recording, was designed and constructed by GeoAnts-GeoDestek LLC to assess axial load along the RAP. During pier installation and load testing, sensor data were monitored in real time using a field data acquisition unit.

This section describes the soil profile of the research site, the preliminary validation tests conducted to finalize the load cell design, the installation of the instrumented Impact® RAP, and the loading tests performed on the instrumented pier.

3.1. Soil Profile Characterization

The instrumented RAP test was conducted at an ongoing pier installation site on the Aegean Sea coast in Milas, Muğla, Türkiye, facilitating easy access for the research team and equipment (Figure 5).

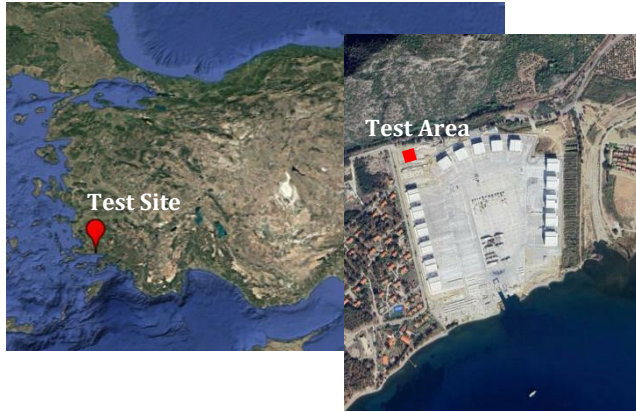


Figure 5. Instrumented RAP Installation Test Site.

Figure 6 presents the variations of SPT N, liquid limit (LL), plastic limit (PL), and water content (ω), with depth, along with the soil profile. The geotechnical soil profile indicates a 1 meter thick upper layer of uncontrolled fill (blocky, clayey, sandy) underlain by sandy, gravelly soft to medium stiff clay layers extending to depths of 11 m. Beneath these, a 4 m thick silty sand gravel layer is followed, by silty medium dense sand down to 20 m. Groundwater is observed at a depth of 2 m.

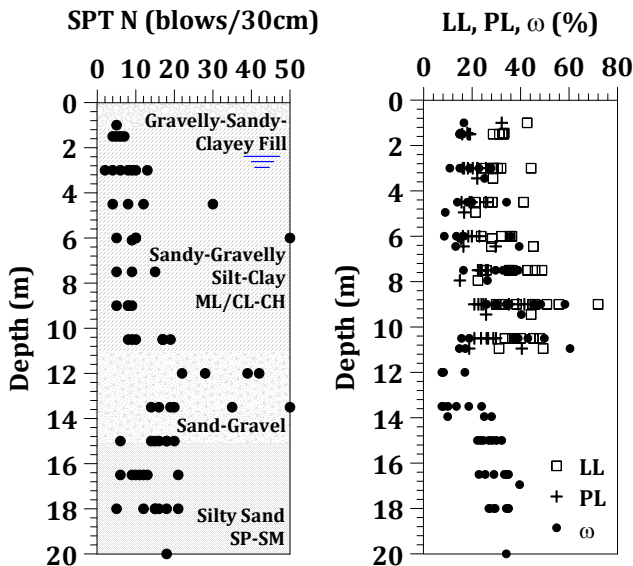


Figure 6. Variation of SPT N, LL, PL, ω Values with Depth Along with the Representative Soil Profile.

The Impact® RAP installation steps are planned to be thoroughly described in order to provide a comprehensive overview of the system technology

prior to proceeding with the load cell design and integration.

3.2. Impact® Rammed Aggregate Pier® Installation

Impact® RAP elements are constructed using displacement methods with a mobil-ram base unit fitted with a high-frequency vibratory hammer. Upon reaching the designed depth with a 36 cm diameter patented chained tamper head and mandrel, aggregate is placed hopper inside, flowing to the mandrel's base. The tamper head and mandrel are then withdrawn approximately 1 meter and driven back down 0.67 m, forming a 0.33 m thick compacted lift. Compaction is achieved through hydraulic crowd pressure and dynamic vertical energy, densifying the aggregate within the displaced cavities to create stiff aggregate pier elements with a final diameter of approximately 50 cm. Figure 7 shows a view from the RAP installation site.

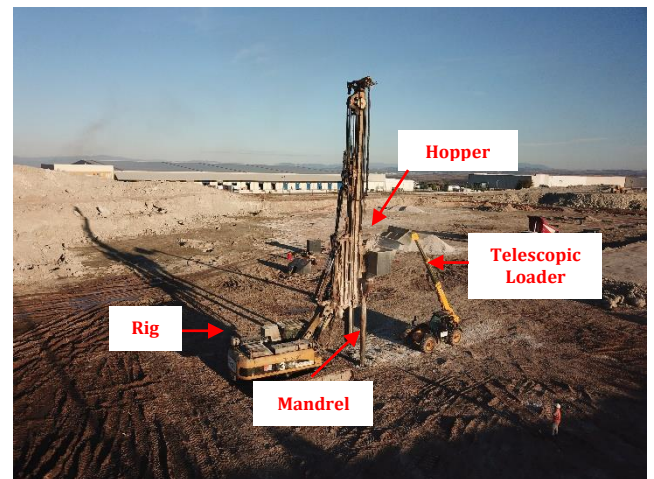


Figure 7. A View from Impact® RAP Installation Site.

3.3. Load Cell Design

A specialized load cell was designed to measure loads at various levels within the pier. Since the Impact® RAP installation involves driving the mandrel into the soil using axial force and vertical vibration, the key focus was to ensure the load cell remains undamaged. A trial study was conducted to assess and mitigate the potential damage to the load cell at the mandrel tip during installation. The mandrel was inserted to a depth of 2 m, the load cell manually lowered to the pier shaft, and the standard RAP installation procedure commenced as compacting the aggregate material above the load cell as shown in Figure 8. After the demo-installation, rapid plate load test was performed to confirm the successful recording of load cell data.

Figure 9 shows that during RAP installation, the total load distribution in the load cell provides a stable load level under dead aggregate loads both during mandrel driving and after the load cell reached the base.

Furthermore, the load cell data recording presented in Figure 9 confirms that the 3-up/3-down (for the bottom bulb-Step 1) and 3-up/2-down (Steps 2-3-4) RAP installation procedure, schematically depicted in Figure 8, was successfully implemented.



Figure 8. Impact® RAP Installation Steps.

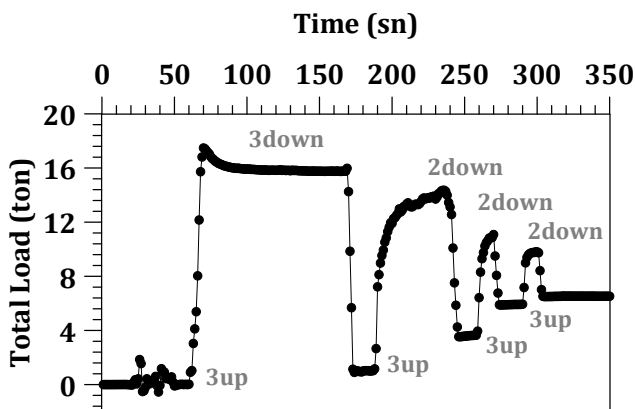


Figure 9. Measured Total Load During RAP Installation.

Figure 10 presents the data recording obtained from the load cell during the plate loading test performed after RAP installation.

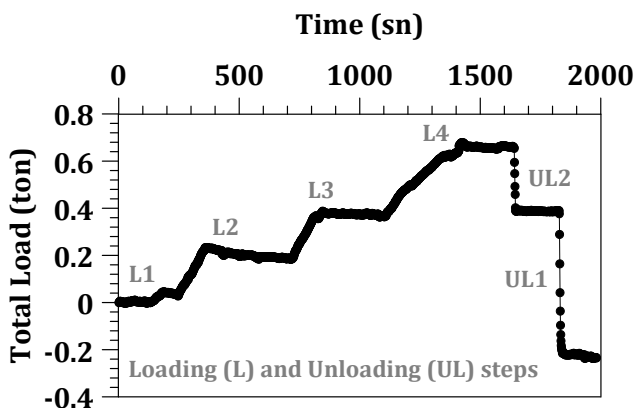


Figure 10. Measured Total Load During Plate Load Test.

The plate loading test involved four incremental loading stages of 5 tons, 10 tons, 15 tons, and 20 tons (Figure 10 - L1 to L4). A linear increase in the load cell data was observed during each loading stage, and data stabilization was confirmed at each load level. Following the loading stages, the load was unloaded in two stages (Figure 10 - UL1 & UL2). Data acquisition continued briefly after the completion of the loading test, and data collection ceased once data stabilization was observed.

The modified load cell was designed with an outer diameter of 33 cm and a height of 13.4 cm (Figure 11). Four independently operating full-bridge resistive strain gauge load cells were placed inside. A 4 mm thick steel around the circumference was implemented to enclose, protect the load cell from water and moisture and withstand damage during mandrel driving with axial force and vertical vibration.



Demo-load cell

- t=10 mm (plate)
- $\phi=46$ cm (plate)
- t=2 mm (cover)

Modified-load cell

- t=12 mm (plate)
- $\phi=33$ cm (plate)
- t= 4 mm (cover)

Figure 11. The Schematic View of the Designed Load Cells: a) Demo-load cell b) Modified-load cell.

Signal cables for each strain gauge channel were routed to the surface through four custom designed tell-tale channels encased in PPRCs sleeves. To measure vertical deformations at the load cell levels, tell-tale bars were also used at the exact locations of the load cells.

Figure 12, Figure 13 and Figure 14, the setup of the tell-tale bars and signal cables at each load cell site is presented. The data from the sensor channels were stored via two specially manufactured 8-channel signal conditioning and digitizing data acquisition units, each with built-in recording capability, and were displayed in real-time using desktop software on-site. At each level, four load cells were positioned to sense the load together, with a total of 16 load cells distributed across four different levels.

At each level, a load cell equipped with four load-measuring sensors was meticulously positioned to ensure that the load cell remained horizontally

oriented without any tilt. For the tilt-meters, a single 4-channel data acquisition unit was used, and the values were displayed in real-time via software, both during the installation of the piers and during load testing. The tilt-meters were used to provide valid information about the final positions of the load cells after placement.

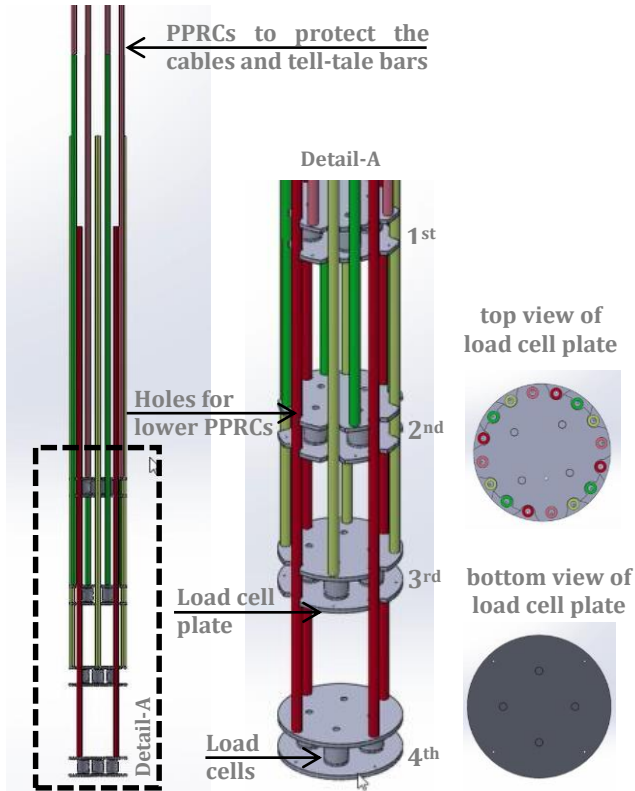


Figure 12. The Schematic View of the Designed Load Cell.



Figure 13. The Photographs from Site of the Designed Load Cell (3rd level).

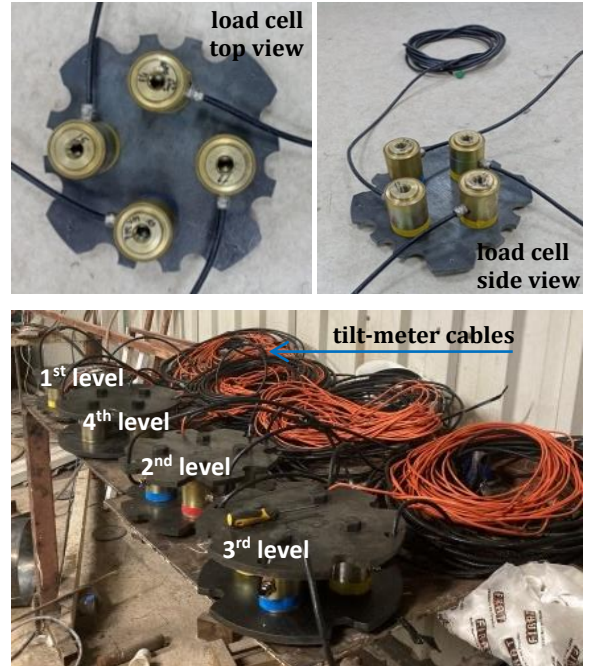


Figure 14. The Photographs from Site of the Designed Load Cell.

3.4. Instrumented Impact[®] RAP Installation

To mitigate granular material collapse during load cell placement, a separate casing was used during pier installation (Figure 15). The installation process for the instrumented test pier involved the following steps: A 40 cm diameter casing was driven to a depth of 6 m using a conical sacrificial plate. A 25 cm diameter mandrel was then lowered to 8 m to install RAP between depths 8 m and 6 m. After retracting the mandrel, the initial load cell was positioned precisely at 6 m. The mandrel was reinserted, and RAP was installed between depths of 6 m and 4 m. Using the same procedures load cells were subsequently placed at depths of 4 m, 2 m, and 1 m, with RAP installations performed between those levels. The process concluded with the final RAP installation reaching the ground surface. Care was taken to avoid damaging the cables, and data was systematically recorded throughout the RAP installation. The load cells remained stable without tilting in any direction.



Figure 15. Some Photos from Instrumented Impact® RAP Installation.

3.5. Full Scale Modulus Load Test on Instrumented Impact® RAP

The full-scale loading test followed the ASTM D-1143 standard to assess load mobilization along the pier. The counterweight included four steel pipes (38 cm diameter) and 60 tons of concrete blocks: two blocks measuring 2 m x 2 m x 1 m and four blocks with a diameter of 2.3 m and thickness of 1 m. A hydraulic jack applied the load, controlled by a 100 ton capacity load cell. Displacement at the top of the column was measured using three dial gauges. However, at the tell-tale elements, out of the sixteen installed gauges, only ten were operational and successfully monitored displacements (three gauges at levels 1, 2, and 3, one gauge at level 4). Load values were recorded at each stage, starting with 5% increments until the maximum load was reached. Measurements continued for the recommended duration, ensuring the settlement rate exceeded 0.254 mm/hour or 0.064 mm/15 minutes. The test lasted 13 hours and 15 minutes. The load test was conducted according to the loading scheme outlined in Table 1. Figure 16 illustrates the loading test setup.

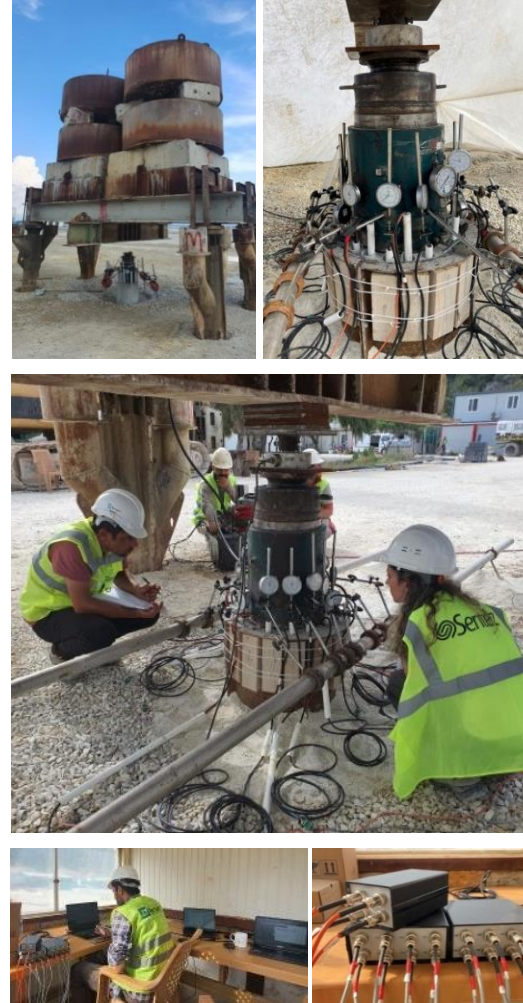


Figure 16. The Instrumented RAP Load Test Setup.

Table 1. Full Scale Modulus Load Test Scheme.

#	Load Cycle (%)	Time (min.) min./max.	Load (ton)	#	Load Cycle (%)	Time (min.) min./max.	Load (ton)
0	5	5/-	1.2	17	100	5/-	25.0
1	16	15/60	4.0	18	133	5/-	33.2
2	33	15/60	8.25	19	150	15/60	37.5
3	50	15/60	12.5	20	175	15/60	43.7
4	66	15/60	16.5	21	200	15/60	50.0
5	83	15/60	20.7	22	230	15/60	57.5
6	100	15/60	25.0	23	150	5/-	37.5
7	115	60/240	28.7	24	100	5/-	25.0
8	133	15/60	33.2	25	66	5/-	16.5
9	150	15/60	37.5	26	33	5/-	8.25
10	133	5/-	33.2	27	0	5/-	0.0
11	100	5/-	25.0	28	100	5/-	25.0
12	66	5/-	16.5	29	200	5/-	50.0
13	33	5/-	8.25	30	264	5/-	66.0
14	0	5/-	0.0	31	276	5/-	69.0
15	33	5/-	8.25	32	0	-	0.0
16	66	5/-	16.5				

4. Results

This section will present the results of the instrumented load test, along with the load cell measurements recorded during the testing process.

4.1. Load Test Results

The loading test was conducted in three cycles, applying loads of 37.5 tons, then to 57.5 tons, and ultimately about 66 tons. Deformations of 47.28 mm, 91.8 mm, and 123.35 mm were recorded at 37.5 tons, 57.5 tons, and 66 tons, respectively. At the final load, the deformation at the top of the RAP increased significantly around 135 mm. Figure 17 illustrates the load-settlement ($q-\delta$) behaviors of the instrumented pier during the test for each load cell levels.

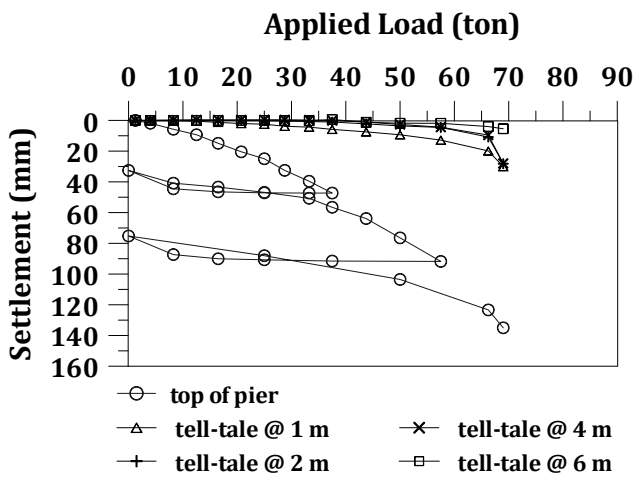


Figure 17. The Applied Load vs. Top-of-Pier Settlement Graphs Including of Tell-Tale Responses for 1st Level (1 m), 2nd Level (2 m), 3rd Level (4 m), and 4th Level (6 m).

Under the 57.5 ton load, displacement at 1 m depth measured about 15% of the top-level displacement, while at depths of 2 m, 4 m, and 6 m, displacements ranged from 5% to 2%. The tell-tale load-settlement curves indicate that bulging deformation predominantly releases during compression. Chen, Han, Oztoprak, and Yang (2009) demonstrated that the settlement ratio, defined as, $R_b = (\delta_{top} - \delta_{tip}) / \delta_{tip}$, supports in evaluating the contributions of both the pier shaft and the underlying soil to the pier's settlement. When $R_b > 1$ settlement mainly arises from the pier's shortening, including bulging and compression. Conversely when $R_b < 1$, the majority of settlement is ascribed to the compression of the soil beneath the pier tip. For the instrumented Impact® RAP element, the settlement ratio is $\gg 1$, and the observed bulging behavior is found to be consistent with the literature. Furthermore, the pier length is sufficiently long for tip behavior to manifest, as indicated by a length to

diameter ratio (L/D) exceeding 3.5, as per Suleiman and White (2006). Pier stiffness decreases sharply for settlements under 20 mm and gradually approaches a minimum asymptote as settlement exceeds 20 mm.

4.2. Load Cell Readings

During the pier installation and loading test, continuous data was collected from the load cells installed at the four levels of the pier. There was no evidence of tilting of the load cells during any of the load cycles. The measured load from load cells along with load cycle times during the loading test is presented in Figure 18. The load distribution recorded by the load cells are shown in Figure 19.

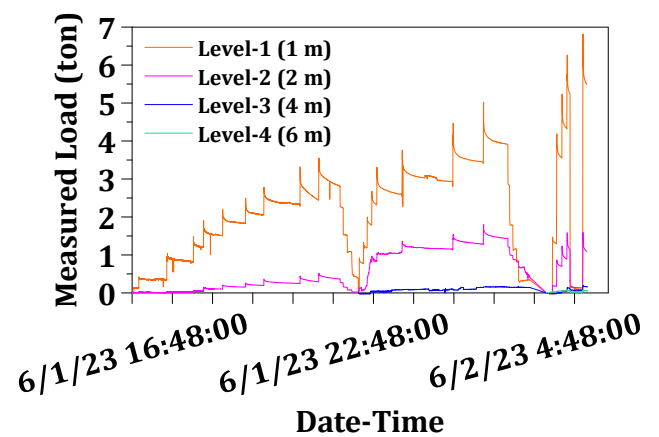


Figure 18. Measurements of Load vs. Load Cycle Time During the Loading Test.

The first (at 1 m) and second (at 2 m) level load cells recorded significant axial loads at the first cycle of the loading which reached up to a maximum load of 37.5 tons. For the second cycle, a small value was recorded at the third level (at 4 m) under 57.5 tons. The fourth level load cell (at 6 m) standard recording data in the third cycle at approximately 66 tons. At 37.5 tons, the vertical load increase at 1 m depth is about 10% of the applied vertical load. The results reveal that most of the load dissipates within the first meter of the pier shaft, with reduced dissipation in the next two meters.

The load is primarily supported by shaft friction instead of being transferred to the pier's tip, indicating higher dissipation occurs within the bulging depth. According to Wissmann (1999), the depth of bulging for an individual column is about 0.9 m, aligning with most of the load being mobilized at $\sim 2D$ depth. Similarly, Chen et al. (2009) characterized the bulging depth as being equal to $2D$, noting that the increase in axial load along the RAP decreases rapidly with increasing depth. This phenomenon suggests that higher lateral resistance acts on the shaft as a result of the installation effect.

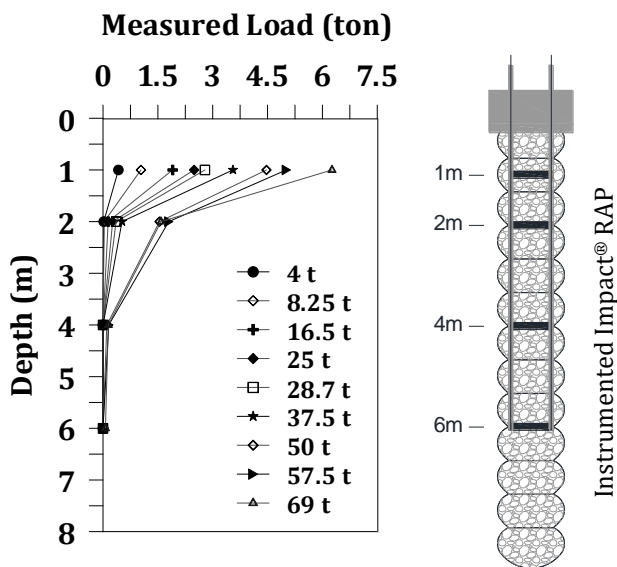


Figure 19. Measurements of Load Distribution Along the RAP During the Loading Test.

5. Discussion

Under working loads, vertical stresses are transmitted through aggregate piers in a manner similar to friction piles, yet with two key distinctions. The majority of the load is transferred through the pier to the adjacent soil matrix through shear stresses at the pier-soil interface, similar to the skin resistance observed in friction piles. However, aggregate piers also develop bearing resistance along the underside of undulations at the pier's perimeter, transferring potential shear surfaces into the matrix soil rather than along the pier-soil interface. This results in greater shear resistance than that which would develop along a regular surface. Additionally, as settlement occurs, deformations near the top of the pier manifest as bulging, displacing the matrix soil outward and increasing lateral pressures along the interface. This heightened lateral pressure enhances the pier's stiffness, resembling the stiffening effect seen in strain-hardening materials.

Research by White, Pham, and Hoevelkamp (2007), Wissmann, White, and Lawton (2007), and Gamboa (2022) examined the load-deformation behavior of RAP, with experimental results compared to existing literature to better understand aggregate pier performance across various soil profiles and column depths. A key distinction is that this study uses a displacement Impact® System yielding a 40 cm final diameter, while the earlier studies employed a replacement method with a 76 cm final diameter. The load-settlement results from White et al. (2007), Wissmann et al. (2007), and Gamboa (2022) align with this study, showing minimal settlement at the column base. This indicates that overall settlement at the

column top is largely due to lateral displacement or bulging of the pier head rather than vertical displacement of the overall column. Gamboa (2022) and others highlight that the density/stiffness of the surrounding soil significantly influence performance, more so than placing the pier tip on a bearing layer, provided the pier is long enough to transfer the load imposed by the concrete cap. Consistent with this study, a sufficiently long pier dissipates stress effectively, with little deformation or stress transfer along the pier length (Gamboa, 2022). A notable difference lies in the load dissipation percentages at similar depths. This study found that at a depth of about two pier diameters ($\sim 2D$), 10% of the applied 37.5 ton load is dissipated. In contrast, at the 2D depth and similar load levels, White et al. (2007) and Gamboa (2022) reported approximately 40% dissipations for a 2.97 m floating pier and a 4.2 m end-bearing column. These columns are significantly shorter than the 8 m pier tested in this study. The discrepancy between the results can be attributed to differences in column length and the resulting end-bearing versus floating behavior of the pile and variations in the strength properties of the surrounding soil. The results suggest that for sufficiently long piers, mobilization occurs primarily through skin friction, with minimal stress transmitted to the column tip. In accordance with literature, the axial load is understood to decrease rapidly along the column with each load increase, particularly within the region extending from the column's bottom elevation to the 2D influence depth. As a summary, the stiffness ratio between the pier and surrounding soil—particularly in the upper 1 meter ($\sim 2D$ depth)—is the most critical factor in load distribution, as most axial load is mobilized in this zone.

The behavior of the RAP element is largely governed by the shear strength and stiffness of the surrounding soil. Most of the load is transmitted from the pier to the soil through shear stress along the pier soil interface, akin to the skin resistance that develops around the perimeter of friction piles. However, the piers also develop bearing resistance along the underside of the undulations at the pier's perimeter, which transfers the potential shear surface into the surrounding soil rather than along the pier soil interface. Consequently, the overall shear resistance is greater than what would develop along a regular surface.

A more rigid native crustal host soil helps create a stiffer pier, which appears to be more effective at dissipating stress and less prone to large bulging or lateral displacements.

The findings indicate that, when determining the capacity and anticipated settlement of aggregate piers, the stiffness of the surrounding soil is more critical

than reaching a bearing layer, provided the pier length is sufficient to dissipate the applied stresses effectively.

6. Conclusion

This study evaluated the design, installation, and full-scale load testing of a specialized load cell used in Impact® RAP (Rammed Aggregate Pier®) installation.

Key findings are as follows:

- The full-scale load test, conducted per ASTM D-1143, applied loads of 37.5, 57.5, and 66 tons in three cycles, recording top displacements of 47.28 mm, 91.8 mm, and approximately 123 mm, respectively. At 57.5 tons, displacement at 1 m depth was about 15% of the top-level displacement, while other levels (2 m, 4 m, and 6 m) showed 2–5% of the top displacement. The settlement ratio ($R_b \gg 1$) indicated that settlement primarily resulted from pier shortening and bulging, consistent with literature.
- A well-instrumented RAP, utilizing load cell and tell-tale bar readings, demonstrated that most axial load (10% of 37.5 tons at 1 m depth) dissipated within the first meter, with minimal load transfer to the pier tip, suggesting dominant shaft friction and minimal tip contribution, consistent with a length to diameter ratio (L/D) greater than 3.5.
- The study highlights that load transfer in aggregate piers occurs mainly through shear stresses at the pier-soil interface, enhanced by bulging-induced lateral pressures. Compared to prior studies, this 8 m pier showed lower load dissipation (10% at $\sim 2D$ depth) than shorter piers (40% at $\sim 2D$). The results emphasize the critical role of the surrounding soil's stiffness particularly in the upper 1 m ($\sim 2D$ depth), in load distribution and pier performance. For sufficiently long piers, load mobilization relies primarily on skin friction, with minimal stress transfer to the pier tip, underscoring the importance of soil stiffness over reaching a bearing layer in design considerations.
- Based on the investigated load transfer mechanisms along the pier shaft, it can be stated that in the design of RAP elements depending on the column length as the influence of shaft friction, with negligible contribution from the pier tip.

The mechanical properties of the surrounding soil significantly influence the behavior of RAP elements. Therefore, more site tests should be conducted on both coarse and fine-grained materials with varying

consistencies to gain a clearer understanding of the load transfer mechanism at the piers.

The instrumented loading test conducted in this study focused on the behavior of a single element, and future studies should be expanded to include understanding the behavior of a group of columns.

Future work will entail a parametric analysis of the collected data, substantiated by finite element simulations and experimental test outcomes.

Acknowledgements

This research has been funded by Sentez Insaat, Istanbul, Türkiye, whose contribution and support for the publication of the project data is greatly appreciated by the authors.

Authorship Contribution Statement

Ece KURT BAL: Developed Methodology, Designed, Planned and Conducted Site Study, Managed Resources, and Wrote the original draft.

Mustafa Kubilay KELEŞOĞLU: Conceptualized the Study, Site Study, Validated Results, Reviewed and Edited Manuscript, and Provided Supervision.

Kemal Önder ÇETİN: Conceptualized the Study, Site Study, Validated Results, Reviewed and Edited Manuscript, and Provided Supervision.

Declaration of Competing Interest

The authors have no conflicts of interest to declare regarding the content of this article.

References

- ASTM D1143 – 81 (Reapproved 1994). Standard test methods for deep foundations under static axial compressive load. Annual Book of ASTM Standards.
- Barksdale, R.D., & Bachus, R.C. (1983). Design and construction of stone columns. Federal Highway Administration, Final Report SCEGIT, 83-104.
- Chen, J.F., Han, J., Oztoprak, S., & Yang, X.M. (2009). Behavior of single rammed aggregate piers considering installation effects. *Comput. Geotech.*, 36(7), 1191-1199.
- Gamboa, W. (2022). Aggregate piers: stress transfer mechanism and construction effect. Master of Science in Civil Engineering, Montana State University, Montana.
- Greenwood, D.A. (1970). Mechanical improvement of soils below ground surfaces. Proceedings of the Ground Engineering Conference, Institution of Civil Engineers, London, 11-22.

- Handy, R.L., & White, D.J. (2006). Stress zones near displacement piers. II: radial cracking and wedging. *J. Geotech. Geoenviron. Eng.*, 10.1061/(ASCE) 1090-0241 (2006) 132: 1(63), 63-71.
- Hughes, J.M.O. & Withers, N.J. (1974). Reinforcing of soft cohesive soils with stone columns. *Ground Engineering*, 7(3), 42-49.
- John, B., Tim., C., Hilary, S., & Michael, B. (2012). ICE manual of geotechnical engineering volume II. geotechnical design construction and verification. Chapter 84: Ground Improvement.
- Lawton, E.C., & Fox, N.S. (1994). Settlement of structures supported on marginal or inadequate soils stiffened with short aggregate piers. *Proc., Vertical and Horizontal Deformations of Foundations and Embankments, Geotechnical Special Publication No. 40, ASCE, College Station, Tex., Vol. 2, 962-974.*
- Lawton, E.C., Fox, N.S., & Handy, R.L. (1994). Control of settlement and uplift of structures using short aggregate piers. *Proceedings of ASCE National Convention, Atlanta, Georgia.*
- Madhav, M.R., & Vitkar, P.P. (1978). Strip footing on weak clay stabilized with a granular trench or pile. *Canadian Geotechnical Journal*, 15(4), 605-609.
- Suleiman, M.T., & White, D.J., (2006). Load transfer in rammed aggregate piers. *Int. J. Geomech.*, 10.1061/(ASCE)1532-3641(2006)6:6(389), 389-398.
- Vesic, A.S. (1972). Expansion of cavities in infinite soil mass, *Journal of Soil Mechanics and Foundation Engineering Division, ASCE, No. SM3, Vol. 98, pp. 265-290.* The design of vibro-replacement. *Ground Engineering*, 31-37.
- White, K.J., Pham, H.T.V., & Hoevelkamp, K.K. (2007). Support mechanisms of rammed aggregate piers. I: Experimental results. *J. Geotech. Geoenviron. Eng.*, 10.1061/(ASCE)1090-0241(2007)133: 12(1503), 1503-1511.
- White, D.J., Wissmann, K.J., Barnes, A.G., & Gaul, A.J. (2002). Embankment support: a comparison of stone column and rammed aggregate pier soil reinforcement. *Transportation Research Board, 81st Annual Meeting, Washington, DC.*
- Wissmann, K.J. (1999). Bearing capacity of Geopier-supported foundation systems. *Technical Bulletin No. 2, Geopier Foundation Company, Inc., Blacksburg, VA, USA.*

- Wissmann, K.J., Ballegooy, S. van, Metcalfe, B.C. Dismuke, J.N., & Anderson, C.K. (2015). Rammed aggregate pier ground improvement as a liquefaction mitigation method in sandy and silty soils. 6th ICEGE, Christchurch, New Zealand.
- Wissmann, K.J., & Fox, N.S. (2000). Design and analysis of short aggregate piers used to reinforce soil for foundation support. *Proceedings, Darmstadt Technical University Colloquium. Germany.*
- Wissmann, K.J., Moser, K., & Pando, M. (2001). Reducing settlement risks in residual piedmont soil using rammed aggregate pier elements. *Proc., Foundations and Ground Improvement, Geotechnical Special Publication No.113, ASCE, Blacksburg, Va, 943-957.*
- Wissmann, K.J., White, D.J., & Lawton, E. (2007). Load test comparisons for rammed aggregate piers and pier groups. *Univ. of Utah, Salt Lake City, Utah.*
- Wong, H.Y. (1975). Vibroflotation- its effect on weak cohesive soils. *Civil Engineering (London), No.82:44-67.*
- McKelvey, D., Sivakumar, V., Bell, A., & Graham, J. (2004). Modelling vibrated stone columns in soft clay. *Proc ICE Geotech Eng 157(3):137-149.*
- Mitchell, J.K. (1981). Soil improvement-state-of-the-art report. *Proceedings of 10th International Conference on Soil Mechanics and Foundation Engineering, Stockholm, Sweden, June 15-19.*
- Naval Facilities Design Command (NAVFAC). (1983). *Design Manual DM 7.2.*